antioxidants

MDPI

Article

The Potential Effects of Quercetin-Loaded Nanoliposomes on Amoxicillin/Clavulanate-Induced Hepatic Damage: Targeting the SIRT1/Nrf2/NF-κB Signaling Pathway and Microbiota Modulation

Mahran Mohamed Abd El-Emam [1], Mahmoud Mostafa [2], Amina A. Farag [3], Heba S. Youssef [4], Azza S. El-Demerdash [5], Heba Bayoumi [6], Mohammed A. Gebba [7,8], Sawsan M. El-Halawani [9], Abdulrahman M. Saleh [10], Amira M. Badr [11,*] and Shorouk El Sayed [12]

1 Department of Biochemistry and Molecular Biology, Faculty of Veterinary Medicine, Zagazig University, Zagazig 44511, Egypt; mmmahran@vet.zu.edu.eg
2 Department of Pharmaceutics, Faculty of Pharmacy, Minia University, Minia 61519, Egypt; mahmoud_mohamed@mu.edu.eg
3 Department of Forensic Medicine and Clinical Toxicology, Faculty of Medicine, Benha University, Banha 13518, Egypt; amina.farag@fmed.bu.edu.eg
4 Department of Physiology, Faculty of Medicine, Benha University, Benha 13518, Egypt; heba.youssef@fmed.bu.edu.eg
5 Laboratory of Biotechnology, Department of Microbiology, Agriculture Research Centre (ARC), Animal Health Research Institute (AHRI), Zagazig 44516, Egypt; dr.azzasalah@yahoo.com
6 Department of Histology and Cell Biology, Faculty of Medicine, Benha University, Benha 13518, Egypt; heba.bayoumi@fmed.bu.edu.eg
7 Department of Anatomy and Embryology, Faculty of Medicine, Benha University, Benha 13518, Egypt; mohammedgebba@gmail.com
8 Department of Anatomy and Embryology, Faculty of Medicine, Merit University, Sohag 82524, Egypt
9 Department of Biotechnology, Urology and Nephrology Center, Mansoura University, Mansoura 35516, Egypt; sawsanelhalawani@mans.edu.eg
10 Pharmaceutical Medicinal Chemistry & Drug Design Department, Faculty of Pharmacy (Boys), Al-Azhar University, Cairo 11884, Egypt; abdo.saleh240@azhar.edu.eg
11 Pharmacology and Toxicology Department, Faculty of Pharmacy, King Saud University, Riyadh P.O. Box 11451, Saudi Arabia
12 Department of Microbiology, Faculty of Veterinary Medicine, Zagazig University, Zagazig 44511, Egypt; shorokelsaid@zu.edu.eg
* Correspondence: amibadr@ksu.edu.sa

Abstract: Amoxicillin/clavulanate (Co-Amox), a commonly used antibiotic for the treatment of bacterial infections, has been associated with drug-induced liver damage. Quercetin (QR), a naturally occurring flavonoid with pleiotropic biological activities, has poor water solubility and low bioavailability. The objective of this work was to produce a more bioavailable formulation of QR (liposomes) and to determine the effect of its intraperitoneal pretreatment on the amelioration of Co-Amox-induced liver damage in male rats. Four groups of rats were defined: control, QR liposomes (QR-lipo), Co-Amox, and Co-Amox and QR-lipo. Liver injury severity in rats was evaluated for all groups through measurement of serum liver enzymes, liver antioxidant status, proinflammatory mediators, and microbiota modulation. The results revealed that QR-lipo reduced the severity of Co-Amox-induced hepatic damage in rats, as indicated by a reduction in serum liver enzymes and total liver antioxidant capacity. In addition, QR-lipo upregulated antioxidant transcription factors SIRT1 and Nrf2 and downregulated liver proinflammatory signatures, including IL-6, IL-1β, TNF-α, NF-κB, and iNOS, with upregulation in the anti-inflammatory one, IL10. QR-lipo also prevented Co-Amox-induced gut dysbiosis by favoring the colonization of *Lactobacillus*, *Bifidobacterium*, and *Bacteroides* over *Clostridium* and *Enterobacteriaceae*. These results suggested that QR-lipo ameliorates Co-Amox-induced liver damage by targeting SIRT1/Nrf2/NF-κB and modulating the microbiota.

check for updates

Citation: Abd El-Emam, M.M.; Mostafa, M.; Farag, A.A.; Youssef, H.S.; El-Demerdash, A.S.; Bayoumi, H.; Gebba, M.A.; El-Halawani, S.M.; Saleh, A.M.; Badr, A.M.; et al. The Potential Effects of Quercetin-Loaded Nanoliposomes on Amoxicillin/Clavulanate-Induced Hepatic Damage: Targeting the SIRT1/Nrf2/NF-κB Signaling Pathway and Microbiota Modulation. *Antioxidants* **2023**, *12*, 1487. https://doi.org/10.3390/antiox12081487

Academic Editor: Montserrat Marí

Received: 23 June 2023
Revised: 16 July 2023
Accepted: 19 July 2023
Published: 25 July 2023

Keywords: Co-Amox-induced hepatotoxicity; quercetin liposomes; quercetin antioxidant activity; SIRT1, Nrf2 and NF-κB targeting; gut dysbiosis

1. Introduction

The liver is a key organ in the process of drug metabolism. In clinical settings, drug-induced liver injury (DILI) is often reported by physicians [1]. Moreover, DILI is caused by exposure to pharmaceuticals, herbal remedies, or other xenobiotics. Antibiotics are frequently accused of causing autoimmune hepatitis, drug-induced liver destruction, and liver failure following transplantation [2]. Research has shown that amoxicillin-clavulanate (co-amoxiclav (Co-Amox)) is the causative agent that is often associated with DILI [3]. Co-Amox is considered a broad-spectrum antibiotic combination composed of the antibiotic amoxicillin, a semimanufactured antibiotic, and an inhibitor for the enzyme β-lactamase called potassium clavulanate. Many drug combinations of amoxicillin and clavulanate have been released globally over time to improve the ease of dosing, the requirements for prescribing, and the recommended treatments for more serious infections or those caused by bacterial resistance to antibiotics [4]. Co-Amox is commonly prescribed for bacterial infections, including sinusitis, otitis, bacterial bronchitis, and pneumonia [5]. Several investigations have indicated that Co-Amox-induced hepatotoxicity may occur, despite the drug's designated conservation aims [6]. The chance of liver damage and hepatotoxicity rises when amoxicillin is administered with a beta-lactamase inhibitor, such as clavulanic acid [7]. In addition, most DILI-related hospitalizations in clinical medicine are caused by Co-Amox. Co-Amox-induced liver damage could be cholestatic, hepatocellular, and/or mixed damage with hypersensitivity symptoms in certain circumstances [8].

Furthermore, evidence suggests that reactive oxygen species (ROS)-induced oxidative damage is crucial in the pathophysiology of Co-Amox-induced hepatocellular injury. When the endogenous antioxidant system is depleted, free radical scavengers become insufficient, resulting in the initiation of negative consequences [8]. Sirtuin1 (SIRT1) is considered a significant factor in DILI development and can influence a variety of biological activities and processes by controlling specific crucial signaling pathways in antistress, autophagy, and DNA repair. It has been suggested that SIRT1, which is a class III histone deacetylase, has protective effects on hepatocytes since it is routinely expressed in hepatic tissue [9]. However, it is downregulated as an effect of hepatocellular damage. Likewise, the reduced hepatic SIRT1 could aggravate DILI primarily by decreasing the nuclear factor E2-related factor 2 (Nrf2), which significantly boosts the expression of antioxidant enzymes [10].

Substantial ROS production can also induce numerous inflammatory factors that trigger inflammatory responses in the liver. The NF-κB signaling pathway plays a major role in the understanding of the mechanism of inflammation [10]. NF-κB is a dimer protein that aids in the production of various proinflammatory cytokines and induces inflammation as a result [11]. Consequently, liver disease prevention and protection are essential. Interest in the potential applications of natural antioxidants as medicinal agents and immune stimulants has been growing [12,13]. Therefore, increasing antioxidant and anti-inflammatory potency and targeting SIRT1 may mitigate DILI by reducing oxidative stress and promoting tissue regeneration.

Microbiota represent a whole organism as they consist of trillions of microbes, composed of different species with diverse taxonomies in humans, including bacteria and fungi [14]. Regulation of intestinal microbiota ecology is multifactorial through microbial, host immune response, environment interaction, and genetic susceptibility. Disturbance in this interaction in genetically susceptible individuals would lead to microbiota dysbiosis [14]. Recently, the role of microbiota dysbiosis not only in the induction of liver disease but also in the fate of disease pathology and therapy has been reported [14,15]. Patients with coeliac disease have been known to develop liver problems, such as nonalcoholic fatty liver disease (NAFLD) and primary biliary cirrhosis [16]. Moreover, the translocation

of buccal microbiota to the gut has been documented in individuals with liver cirrhosis whose innate immune surveillance is impaired [17]. The overuse of antibiotics leads to microbiota dysbiosis and accelerates the evolution of antibiotic-resistant bacteria [18]. Microbiota dysbiosis affects barrier function, microbiota diversity, and metabolite products, and subsequently impairs the efficiency of hepatoprotective substances [16]. Therefore, antibiotics are important in the progression of liver disease pathogenicity. In this respect, introducing natural prebiotics or probiotic substances to be used either as supplements or antibiotic alternatives to modulate gut microbiota composition is an alternative [19,20]. Previous studies have addressed the role of natural flavonoids, including QR, in modulating microbiota and their metabolite composition [21–23].

Quercetin (QR) is a plant flavonoid that is found in a variety of vegetables, fruits, and seeds, including broccoli, onions, soybeans, and peanuts, as well as drinks created from plants, such as tea and wine [24]. Due to its pleiotropic biological properties, including its anti-inflammatory and antioxidant properties, QR has gained more and more attention. QR has been demonstrated to possess pharmacologically proven neuroprotective [25], cardioprotective [26], hepatoprotective, and nephroprotective properties [27]. Furthermore, its potential use in clinical medicine has also recently been reviewed. Additionally, QR is a prospective liver defender since it can directly neutralize superoxide anion, inhibit various superoxide-producing enzymes, including xanthine oxidase, and maintain levels of reduced glutathione [28]. However, despite its medical potential, the clinical use of QR is severely constrained because of its limited bioavailability and reduced water solubility [29]. Therefore, it is crucial to incorporate QR into drug delivery systems that may enhance its bioavailability. Liposomes, a well-known lipid-based drug delivery system, have good biocompatibility, high drug-loading efficiency, controlled release properties, and can potentially encapsulate lipid-soluble [30] and water-soluble [31] molecules. As a result, drugs that are poorly water-soluble, including QR, are more bioavailable upon formulation into liposomal systems [32]. QR might induce hepatoprotection through activation of SIRT1, which is a potent anti-inflammatory factor [33]. The cocrystallized ligand, resveratrol, that binds to the Sirt1 crystal protein (PDB ID: 5BTR), was utilized as a reference to evaluate the potential of QR to bind SIRT1 via docking [34]. QR can imitate resveratrol's action by binding to the activator region of the SIRT1 protein, therefore activating the SIRT1 pathway [35].

However, to our knowledge, there are no reports of the ameliorative effects of QR nanoliposomes on Co-Amox-induced liver damage in male rats in a SIRT1/Nrf2/NF-κB pathway or gut-liver axis-dependent manner. In light of this, the current study was conducted to assess the protective characteristics of QR in the form of liposomes and to identify the potential mechanisms of action.

2. Materials and Methods

2.1. Chemicals

Augmentin® (amoxicillin/clavulanate potassium) powder for suspension (Glaxo Smith Kline, Brantford, UK) was purchased from a public pharmacy in Egypt. Quercetin (95% purity) and cholesterol were provided by Sigma–Aldrich (St. Louis, MO, USA). Phospholipid 90 G was purchased from Lipoid GmbH (Ludwigshafen, Germany). All other chemicals, solvents, and reagents were of the highest purity.

2.2. Animals

Twenty-eight male Sprague-Dawley rats weighing between 160 and 170 g were purchased from the experimental animal's unit of the College of Veterinary Medicine at Zagazig University (Zagazig, Egypt) for this work. The rats were provided with regular laboratory commercial feed and water before the experiment, and acclimatized for two weeks at approximately 25 °C.

2.3. Preparation of a Nanoliposomal Formulation for Quercetin

Quercetin liposomes (QR-lipo) were developed according to the previously disclosed solvent injection approach [36,37]**.** In brief, Phosopholipon 90 G (15.5 mg/mL), cholesterol (1.5 mg/mL), and QR (3 mg/mL) were dissolved in a sufficient volume of absolute ethanol, forming the organic phase. The organic phase was kept under heat in a closed system until used. Ten milliliters (mL) of deionized water were kept under stirring (750 rpm) at 60–70 °C to form the aqueous phase. The organic solution was injected into the aqueous phase using a syringe (25 G needle). QR-lipo production was indicated by the aqueous medium turning into a milky mixture during the injection process. The resulting suspension was maintained at 60 °C for 20–30 min to facilitate ethanol evaporation. The mixture was then stirred continuously for 1–2 h at room temperature and finally stored at 4 °C until further characterization. The resultant liposomal suspension phospholipid concentration is 20 mM containing 20 mM% cholesterol. Encapsulation efficiency (%) of QR was estimated spectrophotometrically (UV-1900, Shimadzu, Kyoto, Japan) at 373 nm after the lysis of liposomal systems as previously described [38]. QR-lipo was evaluated for several parameters, including particle mean diameter, particle charge, polydispersity index, and transmission electron microscopy. The in vitro release profile of QR in the form of liposomes was also examined, as previously reported [30]. An aliquot of QR-lipo was placed in the sample compartment of a Franz diffusion cell. Water and ethanol were mixed in a ratio of 65:35 in the release medium and placed in the reservoir compartment to maintain sink conditions that replicate the in vivo environment [39]. A nitrocellulose membrane with a molecular weight cutoff of 12 to 14 KDa separated the two compartments. System temperature and speed were maintained at 37 °C and 50–60 rpm, respectively. Two mL of the dissolving medium were collected at regular intervals and put through UV analysis at 373 nm to quantify QR using a standard curve. An equal volume of release medium maintained at 37 °C was introduced in the reservoir compartment.

2.4. Experimental Design

Rats were randomly allocated into four groups (n = 7), control group, quercetin liposome-treated group (QR-lipo), the Co-Amox treated group, and the Co-Amox group treated with QR-lipo (Co-Amox and QR-lipo). The liver injury was induced by Co-Amox oral suspension at a dose of 60 mg/kg for ten consecutive days [8]. Rats in the Co-Amox and QR-lipo group received daily doses of 5 mg/kg of QR-lipo intraperitoneally for 10 consecutive days, 1 h before receiving an oral suspension of Co-Amox [37]. Rats in the control group were only given saline solution. Rats in the QR-lipo treatment received daily intraperitoneal injections of 5 mg/kg of QR-lipo for ten days without ingesting Co-Amox. Figure 1 is a schematic diagram summarizing the experimental design.

2.5. Sampling

The rats were sacrificed by carbon dioxide exposure and necropsied 24 h after the last co-amoxiclav treatment. Blood samples were immediately obtained from caudal vena cava before necropsy. After that, the samples used for biochemical research were stored at room temperature in order to isolate serum devoid of anticoagulants. The liver was removed and divided into three parts. After homogenizing a portion in ice-cold phosphate-buffered saline (PBS), the supernatant was utilized to determine the antioxidant status. The second portion was utilized to analyze gene expression using real-time PCR. The remaining liver portion was stored in a 10-percent buffered neutral formalin solution for histological and immunohistochemical analysis.

2.6. Biochemical Analysis

Alanine transaminase (ALT), aspartate transaminase (AST), and total albumin levels were determined by the colorimetric method according to kits supplied by Chema Diagnostica (Monsano, Italy), Tulip Diagnostics (Chennai, India), and Agape Diagnostics (Cham, Switzerland), respectively.

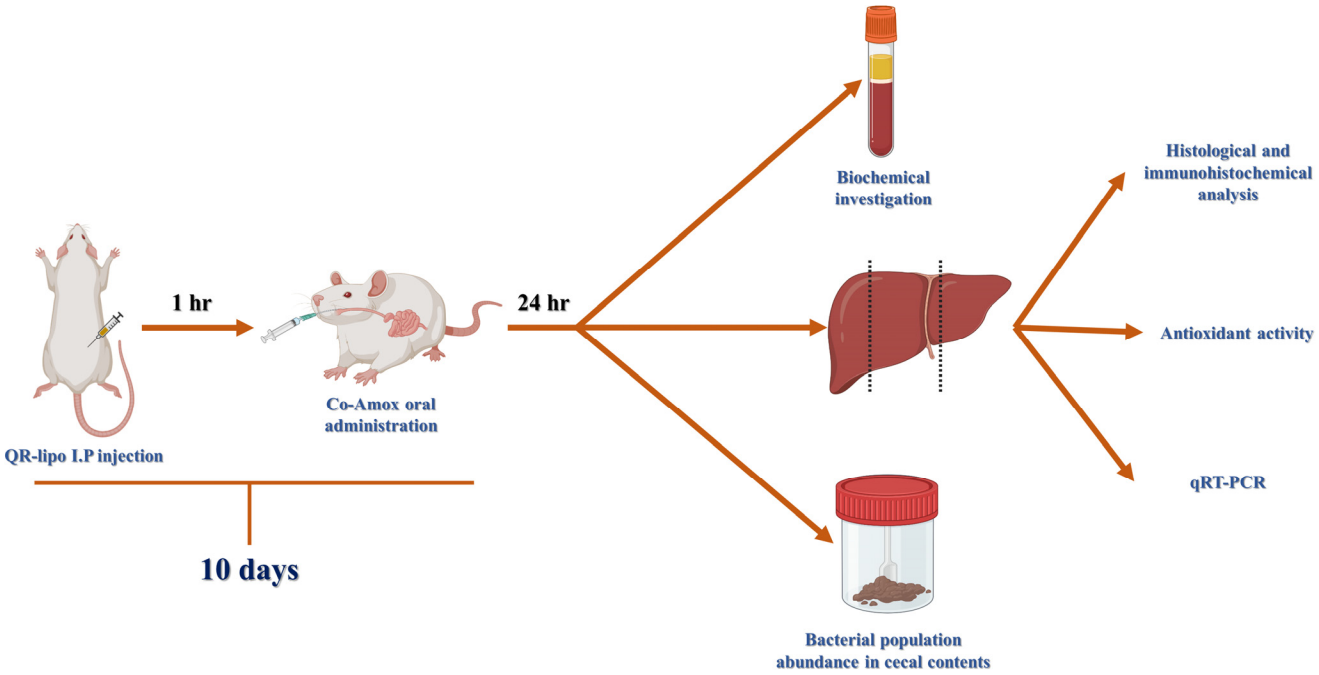

Figure 1. Schematic diagram summarizing the experimental design.

2.7. Determination of the Antioxidant Status

The sample's antioxidants were mixed with a predetermined amount of exogenously generated hydrogen peroxide (H_2O_2) to calculate the liver supernatant's overall antioxidant capacity. The antioxidants in the sample neutralize some of the provided hydrogen peroxide, while the residual H_2O_2 concentration was determined using a calorimetric enzymatic reaction that involved the production of a colored product from 3,5-dichloro-2-hydroxybenzenesulfonate. The total antioxidant level was calculated using the following equation [40]:

$$\text{(Absorbance of blank) - (absorbance of the sample)} \times 3.33\ \text{(mM/L)} \quad (1)$$

Catalase (CAT) activity was estimated calorimetrically in the supernatant by the method described by Hugo Aebi et al. [40]. A catalase inhibitor is used to stop the reaction between a known quantity of H_2O_2 and CAT after exactly one minute. Horseradish peroxidase allowed 3,5-dichloro-2-hydroxybenzene sulfonic acid and 4-aminophenazone to react with the remaining H_2O_2 to produce a chromophore with a color intensity that was inversely correlated to the amount of catalase in the initial sample [40]. Malondialdehyde (MDA) level in liver tissue was determined by the method described by Hiroshi Ohkawa et al. [41]. A thiobarbituric acid (TBA) reactive product was created when TBA and MDA reacted at 95 °C for 30 min in an acidic medium to form a colored product that could be estimated spectrophotometrically at 534 nm. Reduced glutathione (GSH) levels in liver tissue were estimated by the reduction of 5,5-dithiobis (2-nitrobenzoic acid) (DTNB) with GSH to form a yellow-colored chromogen [42]. The absorbance of the resulting chromogen at 405 nm was determined using a commercial kit (Bio Diagnostic, Cairo, Egypt), and it was directly proportional to GSH content.

2.8. mRNA Quantification Using Real-Time RT-PCR

The QIAamp RNeasy Mini kit was used to extract and purify the total RNA from liver tissue in accordance with the manufacturer's instructions (Qiagen, Hilden, Germany). Thermo Fisher Scientific's Nanodrop 8000 was used to assess the amount of total RNA present. A list of the primers used in this work was provided by Metabion (Planegg, Germany), as shown in Table 1. The reaction was carried out in a 25 µL running volume using 10 µL of the

2× HERA SYBR® Green RT-qPCR Master Mix (Willow Fort, Nottinghamshire, UK), 1 µL of the RT Enzyme Mix (20×), 0.5 µL of each primer at a concentration of 20 pmol, 5 µL of RNAse-free water, and 3 µL of RNA template. A step-one real-time PCR instrument was used to conduct the experiment. The reverse transcription procedure was carried out at 50 °C for 30 min, the cDNA was denatured at 94 °C for 15 min, and then 40 cycles of 95 °C for 15 s and 60 °C for 30 s were used in the PCR to achieve amplification. According to the approach outlined by Yuan et al.; [43], in order to evaluate the variation in gene expression on the RNA of the different samples, the Ct of each sample was calculated using the $2^{-\Delta\Delta Ct}$ method and normalized to those of β-actin as the housekeeping gene.

Table 1. Primer sequences used for real-time quantitative reverse transcriptase-polymerase chain reaction (qRT-PCR).

Genes	Primer	Sequence (5′-3′)	Accession Number/References
Keap1	Forward	TGGGCGTGGCAGTGCTCAAC	NM_057152/[44]
	Reverse	GCCCATCGTAGCCTCCTGCG	
Gpx	Forward	GGTGTTCCAGTGCGCAGAT	X12367.1/[45]
	Reverse	AGGGCTTCTATATCGGGTTCGA	
IL-6	Forward	TCCTACCCCAACTTCCAATGCTC	NM_012589.2/[46]
	Reverse	TTGGATGGTCTTGGTCCTTAGCC	
IL-1β	Forward	CACCTCTCAAGCAGAGCACAG	NM_031512.2/[46]
	Reverse	GGGTTCCATGGTGAAGTCAAC	
TNF-α	Forward	AAATGGGCTCCCTCTCATCAGTTC	L19123.1/[46]
	Reverse	TCTGCTTGGTGGTTTGCTACGAC	
IL-10	Forward	GCAGGACTTTAAGGGTTACTTGG	L02926.1/[47]
	Reverse	GGGGAGAAATCGATGACAGC	
NF-κB	Forward	AATTGCCCCGGCAT	XM_342346.4/[48]
	Reverse	TCCCGTAACCGCGTA	
iNOS	Forward	CACCACCCTCCTTGTTCAAC	NM_012611/[49]
	Reverse	CAATCCACAACTCGCTCCAA	
Enterobacteriaceae	Forward	CATTGACGTTACCCGCAGAAGAAGC	CU928145/[50]
	Reverse	CTCTACGAGACTCAAGCTTGC	
Bacteroides	Forward	GAGAGGAAGGTCCCCCAC	NC_003228/[51]
	Reverse	CGCTACTTGGCTGGTTCAG	
Bifidobacterium	Forward	CTC CTG GAA ACG GGT GG	CP001213/[52]
	Reverse	GGT GTT CTT CCC GAT ATC TAC A	
Lactobacillus	Forward	AGCAGTAGGGAATCTTCCA	NC_015213/[53]
	Reverse	CACCGCTACACATGGAG	
Clostridium	Forward	AAAGGAAGATTAATACCGCATAA	KF929215/[54]
	Reverse	ATCTTGCGACCGTACTCCCC	
β-actin	Forward	CCTGCTTGCTGATCCACA	V01217.1/[55]
	Reverse	CTGACCGAGCGTGGCTAG	

2.9. Real-Time Quantitative of Bacterial Population Abundance in Cecal Contents

The bacterial DNA was extracted from cecal contents of all rat groups for detection of microbial abundance of the following bacterial species, including *Lactobacillus*, *Bac-*

teroides, *Enterobacteriaceae*, *Bifidobacterium*, and *Clostridium*, using Strata gene MX3005P quantitative real-time PCR (RT-PCR). Using QIAamp Fast DNA Stool Mini (Qiagen, Hilden, Germany), total DNA from a sample of cecal material was extracted. Using a Nanodrop 2000 spectrophotometer (ThermoFisher Scientific Inc.; Waltham, MA, USA), the purity and concentration of extracted DNA were measured. The samples were frozen at −80 °C for subsequent quantitative PCR analysis. The sequence of the primers for selected bacterial species is mentioned in Table 1. Triplicate analyses for PCR amplification were conducted in a 25 µL reaction containing the following mix: 1 µL of each primer (10 mM), SYBR Green PCR Master Mix (12.5 µL) (Qiagen, Hilden, Germany), sterile PCR-grade water (9.5 µL) and specific genomic DNA (2 µL). For the development of standard curves, genomic DNA obtained from pure bacterial cultures was serially diluted tenfold. The Ct threshold cycle values were then plotted against the bacterial DNA copy counts to generate standard calibration curves. The standard curves represented $\log^{10}$ CFU/gram of the fecal contents and quantified the bacterial concentrations in each DNA sample.

2.10. Histological Examination of the Rat Liver

After obtaining a sample of rat liver, it was promptly fixed in a 10% buffered neutral formalin solution for 48 h, dehydrated in progressively increasing alcohol concentrations, cleaned in xylene, and then embedded in paraffin. Five-µm-thick paraffin slices were generated using a microtome (Leica RM 2155, Milton Keynes, England), and dewaxed sections were stained with hematoxylin and eosin (H and E) [56]. Finally, Leica® microscope and an Am Scope® microscope digital camera were used to take all section photos. The following evaluations of the lesions scoring system were made: 0 = no discernible histological changes, 1 = infrequently mild or focal, 2 = multifocal, and 3 = patchy or diffuse) using a semiquantitative approach [57].

2.11. Immunohistochemical Staining

Deparaffinized 5-µm-thick tissue slices were incubated with 3% H_2O_2 for 30 min, after which they were incubated for 1 h at 37 °C with anti-Nrf2 (GTX103322, Genetex, Alton Pkwy Irvine, CA, USA, 1:100) and anti-SIRT1 (ab110304, Abcam, Waltham, MA, USA, 1:70) reagents, following the manufacturer's instructions. Cross-sections were treated with the secondary antibody HRP Envision kit (DAKO) for 20 min after being rinsed with PBS. The slices were then washed with PBS and given a 10-min incubation with diaminobenzidine (DAB). They were then dehydrated, cleaned in xylene, counterstained with hematoxylin, and cover slipped for microscopic analysis. The analysis was completed using the technique adopted from Elsayed et al. [58]. Seven representative nonoverlapping fields were randomly selected and scanned in order to determine the relative mean Area (%) of positive immunohistochemistry expression levels of Nrf2 and SIRT1 in immunestained sections for each tissue section per sample. Data were gathered for the investigation of tissue sections utilizing a Full HD microscopic imaging system (Leica Microsystems Ltd.; Wetzlar, Germany) run using Leica Application software version 3.7.5 for tissue section analysis.

2.12. Molecular Docking Analysis

Using computer-based chemistry approaches and Resveratrol as a reference (Co-crystallized ligand), the probable activity of QR against the SIRT-1 target site was investigated. At first, the target protein was downloaded from the protein data bank (protein Id: 5BTR). All proteins, QR, and resveratrol were prepared, and an MMFF94 force field minimized energy. The key amino acids (Lys444, Asp292, Ala295, Asp298, and Pro212), which are responsible for the activation of the SIRT1 domain by activator attachment (resveratrol) were identified [34]. After completing the molecular docking, 20 positions were generated. The optimal orientations were then obtained, and affinity scores and RMSD values were compiled [59].

Author Contributions: M.M.A.E.-E. and S.E.S. designed, performed the experiments, analyzed the data, and wrote, reviewed, and edited the manuscript. A.S.E.-D. and M.A.G. performed the experiments and analyzed the data. M.M. prepared the liposomal formulation, performed statistical analysis, and reviewed and edited the manuscript. H.B., A.M.S., S.M.E.-H. and A.M.B. evaluated the data critically reviewed the manuscript. A.A.F. and H.S.Y. wrote, reviewed, and edited the manuscript. All authors have read and agreed to the published version of the manuscript.

Funding: This research was funded by Deputyship for Research and Innovation, 'Ministry of Education' in Saudi Arabia.

Institutional Review Board Statement: The animal study protocol was approved by the Ethics Committee of Zagazig University (Institutional animal care and Use committee) under the number ZU-IACUC/2/F/104/2023 and approved on 30 March 2023.

Informed Consent Statement: Not applicable.

Data Availability Statement: Not applicable.

Acknowledgments: The authors extend their appreciation to the Deputyship for Research and Innovation, "Ministry of Education" in Saudi Arabia for funding this research (IFKSUOR3-234-1).

Conflicts of Interest: The authors declare no conflict of interest.

References

1. Villanueva-Paz, M.L.; Morán, N.; López-Alcántara, C.; Freixo, R.J.; Andrade, M.I.; Lucena, F.J. Cubero, Oxidative stress in drug-induced liver injury (Dili): From mechanisms to biomarkers for use in clinical practice. *Antioxidants* **2021**, *10*, 390. [CrossRef]
2. Nakamura, K.; Kageyama, S.; Ito, T.; Hirao, H.; Kadono, K.; Aziz, A.; Dery, K.J.; Everly, M.J.; Taura, K.; Uemoto, S.; et al. Antibiotic pretreatment alleviates liver transplant damage in mice and humans. *J. Clin. Investig.* **2019**, *129*, 3420–3434. [CrossRef]
3. Chalasani, N.; Bonkovsky, H.L.; Fontana, R.; Lee, W.; Stolz, A.; Talwalkar, J.; Reddy, K.R.; Watkins, P.B.; Navarro, V.; Barnhart, H.; et al. Features and outcomes of 899 patients with drug-induced liver injury: The DILIN prospective study. *Gastroenterology* **2015**, *148*, 1340–1352. [CrossRef]
4. Jamshidi, H.R.; Negintaji, S. Effects of Thymol on Co-amoxiclav-Induced Hepatotoxicity in Rats. *Int. J. Med. Lab.* **2021**, *8*, 44–54. [CrossRef]
5. van Eyk, A.D. Treatment of bacterial respiratory infections. *S. Afr. Fam. Pract.* **2019**, *61*, 8–15. [CrossRef]
6. Shi, J.R.; Liu, J.R.; Li, H.M.; Wang, W.; Zhao, S.Y. Clinical features and therapy of persistent bacterial bronchitis in 31 children. *Chin. J. Pediatr.* **2016**, *54*, 527–530. [CrossRef]
7. Petrov, P.D.; Soluyanova, P.; Sánchez-Campos, S.; Castell, J.V.; Jover, R. Molecular mechanisms of hepatotoxic cholestasis by clavulanic acid: Role of NRF2 and FXR pathways. *Food Chem. Toxicol.* **2021**, *158*, 112664. [CrossRef]
8. El-Kholy, W.M.; Hemieda, F.A.E.; Elabani, G.M. Role of Cinnamon Extract in the Protection against Amoxicillin/Clavulanate-Induced Liver Damage in Rats. *IOSR J. Pharm. Biol. Sci.* **2019**, *14*, 14–21.
9. Liu, X.; Zhao, H.; Luo, C.; Du, D.; Huang, J.; Ming, Q.; Jin, F.; Wang, D.; Huang, W. Acetaminophen Responsive miR-19b Modulates SIRT1/Nrf2 Signaling Pathway in Drug-Induced Hepatotoxicity. *Toxicol. Sci.* **2019**, *170*, 476–488. [CrossRef] [PubMed]
10. Yan, T.; Huang, J.; Nisar, M.F.; Wan, C.; Huang, W. The beneficial roles of SIRT1 in drug-induced liver injury. *Oxid. Med. Cell. Longev.* **2019**, *2019*, 8506195. [CrossRef]
11. Yu, H.; Lin, L.; Zhang, Z.; Zhang, H.; Hu, H. Targeting NF-κB pathway for the therapy of diseases: Mechanism and clinical study. *Signal Transduct. Target. Ther.* **2020**, *5*, 209. [CrossRef] [PubMed]
12. Abou-Zeid, S.M.; Ahmed, A.I.; Awad, A.; Mohammed, W.A.; Metwally, M.M.M.; Almeer, R.; Abdel-Daim, M.M.; Khalil, S.R. Moringa oleifera ethanolic extract attenuates tilmicosin-induced renal damage in male rats via suppression of oxidative stress, inflammatory injury, and intermediate filament proteins mRNA expression. *Biomed. Pharmacother.* **2021**, *133*, 110997. [CrossRef] [PubMed]
13. El Bohi, K.M.; Abdel-Motal, S.M.; Khalil, S.R.; Abd-Elaal, M.M.; Metwally, M.M.M.; Elhady, W.M. The efficiency of pomegranate (*Punica granatum*) peel ethanolic extract in attenuating the vancomycin-triggered liver and kidney tissues injury in rats. *Environ. Sci. Pollut. Res.* **2021**, *28*, 7134–7150. [CrossRef]
14. Llorente, C.; Schnabl, B. The Gut Microbiota and Liver Disease. *Cell. Mol. Gastroenterol. Hepatol.* **2015**, *1*, 275–284. [CrossRef] [PubMed]
15. Chen, T.; Li, R.; Chen, P. Gut Microbiota and Chemical-Induced Acute Liver Injury. *Front. Physiol.* **2021**, *12*, 688780. [CrossRef] [PubMed]
16. Henao-Mejia, J.; Elinav, E.; Jin, C.; Hao, L.; Mehal, W.Z.; Strowig, T.; Thaiss, C.A.; Kau, A.L.; Eisenbarth, S.C.; Jurczak, M.J.; et al. Inflammasome-mediated dysbiosis regulates progression of NAFLD and obesity. *Nature* **2012**, *482*, 179–185. [CrossRef] [PubMed]
17. Qin, N.; Yang, F.; Li, A.; Prifti, E.; Chen, Y.; Shao, L.; Guo, J.; Le Chatelier, E.; Yao, J.; Wu, L.; et al. Alterations of the human gut microbiome in liver cirrhosis. *Nature* **2014**, *513*, 59–64. [CrossRef] [PubMed]

18. Aljazzar, A.; El-Hamid, M.I.A.; El-Malt, R.M.S.; El-Gharreb, W.R.; Abdel-Raheem, S.M.; Ibrahim, A.M.; Abdelaziz, A.M.; Ibrahim, D. Prevalence and Antimicrobial Susceptibility of *Campylobacter* Species with Particular Focus on the Growth Promoting, Immunostimulant and Anti-*Campylobacter jejuni* Activities of Eugenol and Trans-Cinnamaldehyde Mixture in Broiler Chickens. *Animals* **2022**, *12*, 905. [CrossRef]
19. Xu, T.; Hu, S.; Liu, Y.; Sun, K.; Luo, L.; Zeng, L. Hawk Tea Flavonoids as Natural Hepatoprotective Agents Alleviate Acute Liver Damage by Reshaping the Intestinal Microbiota and Modulating the Nrf2 and NF-κB Signaling Pathways. *Nutrients* **2022**, *14*, 3662. [CrossRef]
20. Ismail, H.; Ibrahim, D.; El Sayed, S.; Wahdan, A.; El-Tarabili, R.M.; El-Ghareeb, W.R.; Alhawas, B.A.; Alahmad, B.A.-H.Y.; Abdel-Raheem, S.M.; El-Hamid, M.I.A. Prospective Application of Nanoencapsulated *Bacillus amyloliquefaciens* on Broiler Chickens' Performance and Gut Health with Efficacy against *Campylobacter jejuni* Colonization. *Animals* **2023**, *13*, 775. [CrossRef]
21. Lin, R.; Piao, M.; Song, Y. Dietary Quercetin Increases Colonic Microbial Diversity and Attenuates Colitis Severity in Citrobacter rodentium-Infected Mice. *Front. Microbiol.* **2019**, *10*, 1092. [CrossRef]
22. Shi, T.; Bian, X.; Yao, Z.; Wang, Y.; Gao, W.; Guo, C. Quercetin improves gut dysbiosis in antibiotic-treated mice. *Food Funct.* **2020**, *11*, 8003–8013. [CrossRef]
23. Wang, T.T.; Liu, L.; Deng, J.; Jiang, Y.; Yan, X.; Liu, W. Analysis of the mechanism of action of quercetin in the treatment of hyperlipidemia based on metabolomics and intestinal flora. *Food Funct.* **2023**, *14*, 2112–2127. [CrossRef] [PubMed]
24. Karimi, A.; Naeini, F.; Azar, V.A.; Hasanzadeh, M.; Ostadrahimi, A.; Niazkar, H.R.; Mobasseri, M.; Tutunchi, H. A comprehensive systematic review of the therapeutic effects and mechanisms of action of quercetin in sepsis. *Phytomedicine* **2021**, *86*, 153567. [CrossRef] [PubMed]
25. Moujahed, S.; Ruiz, A.; Hallegue, D.; Sakly, M. Quercetin alleviates styrene oxide-induced cytotoxicity in cortical neurons in vitro via modulation of oxidative stress and apoptosis. *Drug Chem. Toxicol.* **2022**, *45*, 1634–1643. [CrossRef]
26. Wang, G.; Li, Y.; Lei, C.; Lei, X.; Zhu, X.; Yang, L.; Zhang, R. Quercetin exerts antidepressant and cardioprotective effects in estrogen receptor α-deficient female mice via BDNF-AKT/ERK1/2 signaling. *J. Steroid Biochem. Mol. Biol.* **2021**, *206*, 105795. [CrossRef] [PubMed]
27. Soliman, M.M.; Gaber, A.; Alsanie, W.F.; Mohamed, W.A.; Metwally, M.M.M.; Abdelhadi, A.A.; Elbadawy, M.; Shukry, M. Gibberellic acid-induced hepatorenal dysfunction and oxidative stress: Mitigation by quercetin through modulation of antioxidant, anti-inflammatory, and antiapoptotic activities. *J. Food Biochem.* **2022**, *46*, e14069. [CrossRef]
28. Pingili, R.B.; Challa, S.R.; Pawar, A.K.; Toleti, V.; Kodali, T.; Koppula, S. A systematic review on hepatoprotective activity of quercetin against various drugs and toxic agents: Evidence from preclinical studies. *Phytotherapy Res.* **2020**, *34*, 5–32. [CrossRef]
29. Palle, S.; Neerati, P. Quercetin nanoparticles attenuates scopolamine induced spatial memory deficits and pathological damages in rats. *Bull. Fac. Pharmacy, Cairo Univ.* **2017**, *55*, 101–106. [CrossRef]
30. Mostafa, M.; Alaaeldin, E.; Aly, U.F.; Sarhan, H.A. Optimization and Characterization of Thymoquinone-Loaded Liposomes with Enhanced Topical Anti-inflammatory Activity. *AAPS PharmSciTech* **2018**, *19*, 3490–3500. [CrossRef]
31. Khater, S.I.; Almanaa, T.N.; Fattah, D.M.A.; Khamis, T.; Seif, M.M.; Dahran, N.; Alqahtani, L.S.; Metwally, M.M.M.; Mostafa, M.; Albedair, R.A.; et al. Liposome-Encapsulated Berberine Alleviates Liver Injury in Type 2 Diabetes via Promoting AMPK/mTOR-Mediated Autophagy and Reducing ER Stress: Morphometric and Immunohistochemical Scoring. *Antioxidants* **2023**, *12*, 1220. [CrossRef] [PubMed]
32. Che, J.; Najer, A. Europe PMC Funders Group Neutrophils Enable Local and Non-Invasive Liposome Delivery to Inflamed Skeletal Muscle and Ischemic Heart. *Adv. Mater.* **2022**, *32*, 2003598. [CrossRef]
33. Shen, P.; Lin, W.; Ba, X.; Huang, Y.; Chen, Z.; Han, L.; Qin, K.; Huang, Y.; Tu, S. Quercetin-mediated SIRT1 activation attenuates collagen-induced mice arthritis. *J. Ethnopharmacol.* **2021**, *279*, 114213. [CrossRef]
34. Cao, D.; Wang, M.; Qiu, X.; Liu, D.; Jiang, H.; Yang, N.; Xu, R.-M. Structural basis for allosteric, substrate-dependent stimulation of SIRT1 activity by resveratrol. *Genes Dev.* **2015**, *29*, 1316–1325. [CrossRef] [PubMed]
35. Iside, C.; Scafuro, M.; Nebbioso, A.; Altucci, L. SIRT1 Activation by Natural Phytochemicals: An Overview. *Front. Pharmacol.* **2020**, *11*, 1225. [CrossRef] [PubMed]
36. Toniazzo, T.; Peres, M.S.; Ramos, A.P.; Pinho, S.C. Encapsulation of quercetin in liposomes by ethanol injection and physicochemical characterization of dispersions and lyophilized vesicles. *Food Biosci.* **2017**, *19*, 17–25. [CrossRef]
37. Alaaeldin, E.; Mostafa, M.; Mansour, H.F.; Soliman, G.M. Spanlastics as an efficient delivery system for the enhancement of thymoquinone anticancer efficacy: Fabrication and cytotoxic studies against breast cancer cell lines. *J. Drug Deliv. Sci. Technol.* **2021**, *65*, 102725. [CrossRef]
38. Odeh, F.; Ismail, S.I.; Abu-Dahab, R.; Mahmoud, I.S.; Al Bawab, A. Thymoquinone in liposomes: A study of loading efficiency and biological activity towards breast cancer. *Drug Deliv.* **2012**, *19*, 371–377. [CrossRef]
39. Huang, J.; Wang, Q.; Chu, L.; Xia, Q. Liposome-chitosan hydrogel bead delivery system for the encapsulation of linseed oil and quercetin: Preparation and in vitro characterization studies. *LWT* **2020**, *117*, 108615. [CrossRef]
40. Aebi, H. Catalase in vitro. In *Methods in Enzymology*; Academic Press: Cambridge, MA, USA, 1984; pp. 121–126. [CrossRef]
41. Ohkawa, H.; Ohishi, N.; Yagi, K. Assay for lipid peroxides in animal tissues by thiobarbituric acid reaction. *Anal. Biochem.* **1979**, *95*, 351–358. [CrossRef]
42. Tietze, F. Enzymic method for quantitative determination of nanogram amounts of total and oxidized glutathione: Applications to mammalian blood and other tissues. *Anal. Biochem.* **1969**, *27*, 502–522. [CrossRef]

43. Yuan, J.S.; Reed, A.; Chen, F.; Stewart, C.N., Jr. Statistical analysis of real-time PCR data. *BMC Bioinform.* **2006**, *7*, 85. [CrossRef] [PubMed]
44. Zhong, Q.; Mishra, M.; Kowluru, R.A. Transcription Factor Nrf2-Mediated Antioxidant Defense System in the Development of Diabetic Retinopathy. *Investig. Opthalmology Vis. Sci.* **2013**, *54*, 3941–3948. [CrossRef] [PubMed]
45. Al-Rejaie, S.S.; Aleisa, A.M.; Sayed-Ahmed, M.M.; Al-Shabanah, O.A.; Abuohashish, H.M.; Ahmed, M.M.; Al-Hosaini, K.A.; Hafez, M.M. Protective effect of rutin on the antioxidant genes expression in hypercholestrolemic male Westar rat. *BMC Complement. Altern. Med.* **2013**, *13*, 136. [CrossRef]
46. Peinnequin, A.; Mouret, C.; Birot, O.; Alonso, A.; Mathieu, J.; Clarençon, D.; Agay, D.; Chancerelle, Y.; Multon, E. Rat pro-inflammatory cytokine and cytokine related mRNA quantification by real-time polymerase chain reaction using SYBR green. *BMC Immunol.* **2004**, *5*, 3. [CrossRef]
47. O'Bryan, M.K.; Gerdprasert, O.; Nikolic-Paterson, D.J.; Meinhardt, A.; Muir, J.A.; Foulds, L.M.; Phillips, D.J.; de Kretser, D.M.; Hedger, M.P. Cytokine profiles in the testes of rats treated with lipopolysaccharide reveal localized suppression of inflammatory responses. *Am. J. Physiol. Integr. Comp. Physiol.* **2005**, *288*, R1744–R1755. [CrossRef]
48. Habibi, F.; Soufi, F.G.; Ghiasi, R.; Khamaneh, A.M.; Alipour, M.R. Alteration in Inflammation-related miR-146a Expression in NF-KB Signaling Pathway in Diabetic Rat Hippocampus. *Adv. Pharm. Bull.* **2016**, *6*, 99–103. [CrossRef] [PubMed]
49. Sobajima, S.; Shimer, A.L.; Chadderdon, R.C.; Kompel, J.F.; Kim, J.S.; Gilbertson, L.G.; Kang, J.D. Quantitative analysis of gene expression in a rabbit model of intervertebral disc degeneration by real-time polymerase chain reaction. *Spine J.* **2005**, *5*, 14–23. [CrossRef]
50. Bartosch, S.; Fite, A.; Macfarlane, G.T.; McMurdo, M.E.T. Characterization of Bacterial Communities in Feces from Healthy Elderly Volunteers and Hospitalized Elderly Patients by Using Real-Time PCR and Effects of Antibiotic Treatment on the Fecal Microbiota. *Appl. Environ. Microbiol.* **2004**, *70*, 3575–3581. [CrossRef]
51. Layton, A.; McKay, L.; Williams, D.; Garrett, V.; Gentry, R.; Sayler, G. Development of *Bacteroides* 16S rRNA Gene TaqMan-Based Real-Time PCR Assays for Estimation of Total, Human, and Bovine Fecal Pollution in Water. *Appl. Environ. Microbiol.* **2006**, *72*, 4214–4224. [CrossRef]
52. Requena, T.; Burton, J.; Matsuki, T.; Munro, K.; Simon, M.A.; Tanaka, R.; Watanabe, K.; Tannock, G.W. Identification, Detection, and Enumeration of Human *Bifidobacterium* Species by PCR Targeting the Transaldolase Gene. *Appl. Environ. Microbiol.* **2002**, *68*, 2420–2427. [CrossRef] [PubMed]
53. Rinttila, T.; Kassinen, A.; Malinen, E.; Krogius, L.; Palva, A. Development of an extensive set of 16S rDNA-targeted primers for quantification of pathogenic and indigenous bacteria in faecal samples by real-time PCR. *J. Appl. Microbiol.* **2004**, *97*, 1166–1177. [CrossRef] [PubMed]
54. Mirhosseini, S.Z.; Seidavi, A.; Shivazad, M.; Chamani, M.; Sadeghi, A.A.; Pourseify, R. Detection of Clostridium sp. and its Relation to Different Ages and Gastrointestinal Segments as Measured by Molecular Analysis of 16S rRNA Genes. *Braz. Arch. Biol. Technol.* **2010**, *53*, 69–76. [CrossRef]
55. Patel, T.P.; Soni, S.; Parikh, P.; Gosai, J.; Chruvattil, R.; Gupta, S. Swertiamarin: An Active Lead from *Enicostemma littorale* Regulates Hepatic and Adipose Tissue Gene Expression by Targeting PPAR-$\gamma$and Improves Insulin Sensitivity in Experimental NIDDM Rat Model. *Evidence-Based Complement. Altern. Med.* **2013**, *2013*, 358673. [CrossRef]
56. Suvarna, K.S.; Layton, C.; Bancroft, J.D. *Bancroft's Theory and Practice of Histological Techniques*, 8th ed.; E. Book Elsevier Health Sciences: Amsterdam, The Netherlands, 2008.
57. Gibson-Corley, K.N.; Olivier, A.K.; Meyerholz, D.K. Principles for Valid Histopathologic Scoring in Research. *Vet. Pathol.* **2013**, *50*, 1007–1015. [CrossRef]
58. Elsayed, H.E.; Ebrahim, H.Y.; Mady, M.S.; Khattab, M.A.; El-Sayed, E.K.; Moharram, F.A. Ethnopharmacological impact of *Melaleuca rugulosa* (Link) Craven leaves extract on liver inflammation. *J. Ethnopharmacol.* **2022**, *292*, 115215. [CrossRef]
59. El Sayed, A.M.; El Hawary, S.; Elimam, H.; Saleh, A.M.; Zokalih, A.H.; Mohyeldin, M.M.; Bassam, S.M. ESI-LC-MS/MS based comparative multivariate metabolomic and biological profiling with dynamic molecular docking of Gmelina arborea Roxb different organs. *Fitoterapia* **2023**, *168*, 105540. [CrossRef] [PubMed]
60. Zhang, X.; Deng, Y.; Hu, S.; Hu, X.; Ma, J.; Hu, J.; Hu, B.; He, H.; Li, L.; Liu, H.; et al. Comparative analysis of amino acid content and protein synthesis-related genes expression levels in breast muscle among different duck breeds/strains. *Poult. Sci.* **2023**, *102*, 102277. [CrossRef] [PubMed]
61. Appiah, J.; Prasad, A.; Shah, V.; Patel, V.; Fareen, N.; Marin, A.C.; Cheriyath, P. Amoxicillin-Clavulanate Induced Liver Injury in a Young Female. *Cureus* **2023**, *15*, e33445. [CrossRef]
62. Byrne, N.J.; Rajasekaran, N.S.; Abel, E.D.; Bugger, H. Therapeutic potential of targeting oxidative stress in diabetic cardiomyopathy. *Free. Radic. Biol. Med.* **2021**, *169*, 317–342. [CrossRef]
63. Akbarian, A.; Michiels, J.; DeGroote, J.; Majdeddin, M.; Golian, A.; De Smet, S. Association between heat stress and oxidative stress in poultry; mitochondrial dysfunction and dietary interventions with phytochemicals. *J. Anim. Sci. Biotechnol.* **2016**, *7*, 37. [CrossRef] [PubMed]
64. Yaman, S.O.; Ayhanci, A. *Lipid Peroxidation*; IntechOpen: London, UK, 2021; pp. 1–11. [CrossRef]
65. Delemos, A.S.; Ghabril, M.; Rockey, D.C.; Gu, J.; Barnhart, H.X.; Fontana, R.J.; Kleiner, D.E.; Bonkovsky, H.L. Amoxicillin–Clavulanate-Induced Liver Injury. *Dig. Dis. Sci.* **2016**, *61*, 2406–2416. [CrossRef] [PubMed]

66. Li, D.; Shi, W.; Lu, X.; Liu, Z.; Zhang, S.; Sun, Y.; Zhu, X. A Protective Role of Okadaic Acid in Liver Injury Induced by Amoxicillin. *Bull. Exp. Biol. Med.* **2022**, *172*, 328–331. [CrossRef] [PubMed]
67. Yang, D.; Tan, X.; Lv, Z.; Liu, B.; Baiyun, R.; Lu, J.; Zhang, Z. Regulation of Sirt1/Nrf2/TNF-α signaling pathway by luteolin is critical to attenuate acute mercuric chloride exposure induced hepatotoxicity. *Sci. Rep.* **2016**, *6*, 37157. [CrossRef] [PubMed]
68. Sun, X.; Wang, P.; Yao, L.-P.; Wang, W.; Gao, Y.-M.; Zhang, J.; Fu, Y.-J. Paeonol alleviated acute alcohol-induced liver injury via SIRT1/Nrf2/NF-κB signaling pathway. *Environ. Toxicol. Pharmacol.* **2018**, *60*, 110–117. [CrossRef]
69. Zhang, Y.; Liang, J.; Cao, N.; Gao, J.; Song, L.; Tang, X. Coal dust nanoparticles induced pulmonary fibrosis by promoting inflammation and epithelial-mesenchymal transition via the NF-κB/NLRP3 pathway driven by IGF1/ROS-mediated AKT/GSK3β signals. *Cell Death Discov.* **2022**, *8*, 500. [CrossRef]
70. Yu, Z.; Guo, F.; Zhang, Z.; Luo, X.; Tian, J.; Li, H. Protective Effects of Glycyrrhizin on LPS and Amoxicillin/Potassium Clavulanate-Induced Liver Injury in Chicken. *Pak. Vet. J.* **2017**, *37*, 13–18.
71. Afifi, N.A.; Ibrahim, M.A.; Galal, M.K. Hepatoprotective influence of quercetin and ellagic acid on thioacetamide-induced hepatotoxicity in rats. *Can. J. Physiol. Pharmacol.* **2018**, *96*, 624–629. [CrossRef]
72. Liu, L.; Liu, Y.; Cheng, X.; Qiao, X. The Alleviative Effects of Quercetin on Cadmium-Induced Necroptosis via Inhibition ROS/iNOS/NF-κB Pathway in the Chicken Brain. *Biol. Trace Element Res.* **2021**, *199*, 1584–1594. [CrossRef]
73. Zheng, Y.; Haworth, I.S.; Zuo, Z.; Chow, M.S.; Chow, A.H. Physicochemical and Structural Characterization of Quercetin-β-Cyclodextrin Complexes. *J. Pharm. Sci.* **2005**, *94*, 1079–1089. [CrossRef]
74. Tang, L.; Li, K.; Zhang, Y.; Li, H.; Li, A.; Xu, Y.; Wei, B. Quercetin liposomes ameliorate streptozotocin-induced diabetic nephropathy in diabetic rats. *Sci. Rep.* **2020**, *10*, 2440. [CrossRef] [PubMed]
75. Yang, H.; Yang, T.; Heng, C.; Zhou, Y.; Jiang, Z.; Qian, X.; Du, L.; Mao, S.; Yin, X.; Lu, Q. Quercetin improves nonalcoholic fatty liver by ameliorating inflammation, oxidative stress, and lipid metabolism in db/db mice. *Phytother. Res.* **2019**, *33*, 3140–3152. [CrossRef] [PubMed]
76. Alqahtani, S.M.; Dawood, A.F.; Kamar, S.S.; Haidara, M.A.; ShamsEldeen, A.M.; Dallak, M.; Al-Ani, B.; Ebrahim, H.A. Quercetin and Resveratrol are Associated with the Downregulation of TNF-α/NF-kB/iNOS Axis-Mediated Acute Liver Injury in Rats Induced by Paracetamol Poisoning. *Int. J. Morphol.* **2023**, *41*, 79–84. [CrossRef]
77. Ehteshamfar, S.; Akhbari, M.; Afshari, J.T.; Seyedi, M.; Nikfar, B.; Shapouri-Moghaddam, A.; Ghanbarzadeh, E.; Momtazi-Borojeni, A.A. Anti-inflammatory and immune-modulatory impacts of berberine on activation of autoreactive T cells in autoimmune inflammation. *J. Cell. Mol. Med.* **2020**, *24*, 13573–13588. [CrossRef] [PubMed]
78. Hussein, R.M.; Sawy, D.M.; Kandeil, M.A.; Farghaly, H.S. Chlorogenic acid, quercetin, coenzyme Q10 and silymarin modulate Keap1-Nrf2/heme oxygenase-1 signaling in thioacetamide-induced acute liver toxicity. *Life Sci.* **2021**, *277*, 119460. [CrossRef] [PubMed]
79. Ahmed, O.M.; Elkomy, M.H.; Fahim, H.I.; Ashour, M.B.; Naguib, I.A.; Alghamdi, B.S.; Mahmoud, H.U.R.; Ahmed, N.A. Rutin and Quercetin Counter Doxorubicin-Induced Liver Toxicity in Wistar Rats via Their Modulatory Effects on Inflammation, Oxidative Stress, Apoptosis, and Nrf2. *Oxidative Med. Cell. Longev.* **2022**, *2022*, 2710607. [CrossRef]
80. Liu, P.; Li, J.; Liu, M.; Zhang, M.; Xue, Y.; Zhang, Y.; Han, X.; Jing, X.; Chu, L. Hesperetin modulates the Sirt1/Nrf2 signaling pathway in counteracting myocardial ischemia through suppression of oxidative stress, inflammation, and apoptosis. *Biomed. Pharmacother.* **2021**, *139*, 111552. [CrossRef]
81. Arioz, B.I.; Taştan, B.; Tarakcioglu, E.; Tufekci, K.U.; Olcum, M.; Ersoy, N.; Bagriyanik, A.; Genc, K.; Genc, S. Melatonin Attenuates LPS-Induced Acute Depressive-Like Behaviors and Microglial NLRP3 Inflammasome Activation Through the SIRT1/Nrf2 Pathway. *Front. Immunol.* **2019**, *10*, 1511. [CrossRef]
82. Atici, B.; Uyumlu, A.B.; Taslidere, A. The role of Nrf2/SIRT1 pathway in the hepatoprotective effect of PEITC against HFD/STZ-induced diabetic liver disease. *Ann. Med. Res.* **2022**, *12*, 1348–1353.
83. Liu, C.-M.; Ma, J.-Q.; Xie, W.-R.; Liu, S.-S.; Feng, Z.-J.; Zheng, G.-H.; Wang, A.-M. Quercetin protects mouse liver against nickel-induced DNA methylation and inflammation associated with the Nrf2/HO-1 and p38/STAT1/NF-κB pathway. *Food Chem. Toxicol.* **2015**, *82*, 19–26. [CrossRef]
84. Zhao, P.; Hu, Z.; Ma, W.; Zang, L.; Tian, Z.; Hou, Q. Quercetin alleviates hyperthyroidism-induced liver damage via Nrf2 Signaling pathway. *Biofactors* **2020**, *46*, 608–619. [CrossRef] [PubMed]
85. Zhang, Y.; Qu, X.; Gao, H.; Zhai, J.; Tao, L.; Sun, J.; Song, Y.; Zhang, J. Quercetin attenuates NLRP3 inflammasome activation and apoptosis to protect INH-induced liver injury via regulating SIRT1 pathway. *Int. Immunopharmacol.* **2020**, *85*, 106634. [CrossRef]
86. Ciccone, L.; Piragine, E.; Brogi, S.; Camodeca, C.; Fucci, R.; Calderone, V.; Nencetti, S.; Martelli, A.; Orlandini, E. Resveratrol-like Compounds as SIRT1 Activators. *Int. J. Mol. Sci.* **2022**, *23*, 15105. [CrossRef] [PubMed]
87. Mi, W.; Hu, Z.; Xu, L.; Bian, X.; Lian, W.; Yin, S.; Zhao, S.; Gao, W.; Guo, C.; Shi, T. Quercetin positively affects gene expression profiles and metabolic pathway of antibiotic-treated mouse gut microbiota. *Front. Microbiol.* **2022**, *13*, 983358. [CrossRef]
88. Yassour, M.; Lim, M.Y.; Yun, H.S.; Tickle, T.L.; Sung, J.; Song, Y.-M.; Lee, K.; Franzosa, E.A.; Morgan, X.C.; Gevers, D.; et al. Sub-clinical detection of gut microbial biomarkers of obesity and type 2 diabetes. *Genome Med.* **2016**, *8*, 17. [CrossRef]
89. Porras, D.; Nistal, E.; Martínez-Flórez, S.; Pisonero-Vaquero, S.; Olcoz, J.L.; Jover, R.; González-Gallego, J.; García-Mediavilla, M.V.; Sánchez-Campos, S. Protective effect of quercetin on high-fat diet-induced non-alcoholic fatty liver disease in mice is mediated by modulating intestinal microbiota imbalance and related gut-liver axis activation. *Free. Radic. Biol. Med.* **2017**, *102*, 188–202. [CrossRef]

90. Xie, J.; Song, W.; Liang, X.; Zhang, Q.; Shi, Y.; Liu, W.; Shi, X. Protective effect of quercetin on streptozotocin-induced diabetic peripheral neuropathy rats through modulating gut microbiota and reactive oxygen species level. *Biomed. Pharmacother.* **2020**, *127*, 110147. [CrossRef]
91. Li, X.; Wang, E.; Yin, B.; Fang, D.; Chen, P.; Wang, G.; Zhao, J.; Zhang, H.; Chen, W. Effects of *Lactobacillus casei* CCFM419 on insulin resistance and gut microbiota in type 2 diabetic mice. *Benef. Microbes* **2017**, *8*, 421–432. [CrossRef]
92. Gryaznova, M.; Dvoretskaya, Y.; Burakova, I.; Syromyatnikov, M.; Popov, E.; Kokina, A.; Mikhaylov, E.; Popov, V. Dynamics of Changes in the Gut Microbiota of Healthy Mice Fed with Lactic Acid Bacteria and Bifidobacteria. *Microorganisms* **2022**, *10*, 1020. [CrossRef] [PubMed]
93. Schulthess, J.; Pandey, S.; Capitani, M.; Rue-Albrecht, K.C.; Arnold, I.; Franchini, F.; Chomka, A.; Ilott, N.E.; Johnston, D.G.W.; Pires, E.; et al. The Short Chain Fatty Acid Butyrate Imprints an Antimicrobial Program in Macrophages. *Immunity* **2019**, *50*, 432–445.e437. [CrossRef]